RP Current Trends In Applied Sciences (e-ISSN: 2583-7486)
Vol. 5, No. 1 (January – March 2026) pp. 32–37

RESEARCH PLATEAU PUBLISHERS

Cite this article: C. Kumari, P.K. Vishwakarma, Structural and optical behaviors of Dy^{3+} activated $BaNb_2O_6$ phosphors for white LED applications, *RP Cur. Tr. Appl. Sci.* **5** (2026) 32–37.

Original Research Article

Structural and optical behaviors of Dy^{3+} activated $BaNb_2O_6$ phosphors for white LED applications

Chandni Kumari[1,*], Praveen Kumar Vishwakarma[2]

[1]Department of Physics, Indian Institute of Technology (Indian School of Mines), Dhanbad Jharkhand - 826004, India
[2]Department of Physics, Patna University, Patna, Bihar - 800005, India
*Corresponding author, E-mail: chand02iitism@gmail.com

ARTICLE HISTORY
Received: 15 April 2026
Revised: 27 May 2026
Accepted: 27 May 2026
Published: 12 June 2026

KEYWORDS
Dy^{3+} - doped phosphors;
Photoluminescence;
White light emission;
Structural and optical properties.

ABSTRACT

Dy^{3+} - activated $BaNb_2O_6$ phosphors were successfully synthesized via a conventional high - temperature solid - state reaction route and systematically investigated for their structural, optical, and photometric properties. X-ray diffraction (XRD) analysis confirmed the formation of a single-phase orthorhombic crystal structure without the presence of any secondary phases, indicating the successful substitution of Dy^{3+} ions into the host lattice. Fourier transform infrared (FTIR) spectroscopy revealed the formation of NbO_6 octahedral units, confirming the structural integrity of the material. UV - Vis diffuse reflectance spectroscopy (DRS) demonstrated strong absorption in the ultraviolet region, and the optical band gap was found to vary from 3.39 to 3.62 eV with increasing Dy^{3+} concentration. Photoluminescence (PL) studies exhibited characteristic emissions corresponding to Dy^{3+} transitions in the blue (~480 nm) and yellow (~575 nm) regions, resulting in near-white light emission. The emission intensity increased up to 1 mol% Dy^{3+} and subsequently decreased due to concentration quenching caused by non-radiative energy transfer. The decay curves followed a single exponential behavior with lifetimes in the range of 0.09 - 0.1 ms. Chromaticity analysis revealed that the phosphors emit in the cool white region with a color purity below 10% and correlated color temperature (CCT) values exceeding 5000 K. These results demonstrate that Dy^{3+} - doped $BaNb_2O_6$ phosphors are promising candidates for solid-state lighting applications.

1. Introduction

The rapid evolution of solid-state lighting technologies has significantly influenced modern illumination systems due to their superior energy efficiency, environmental sustainability, and extended operational lifetime [1,2]. Among these technologies, white light-emitting diodes (WLEDs) have emerged as a dominant lighting source for applications ranging from general illumination to advanced display systems. A crucial component of WLEDs is the phosphor material, which converts high-energy excitation (UV or blue light) into visible light through photoluminescence [2]. Therefore, the development of efficient and stable phosphor materials is essential for improving the performance of WLED devices.

Rare-earth-ion-doped phosphors have attracted considerable attention due to their unique optical properties arising from intra-configurational 4f - 4f transitions. These transitions are shielded by outer 5s and 5p orbitals, resulting in sharp emission lines, high color purity, and excellent thermal stability [1]. Among various rare-earth ions, dysprosium (Dy^{3+}) is particularly significant because it exhibits dual emission bands in the blue and yellow regions, corresponding to the $^4F_{9/2} \rightarrow {}^6H_j$ transitions, respectively [3]. The combination of these emissions can generate near-white light without requiring multiple dopants, simplifying device fabrication and improving color stability.

The host lattice plays a critical role in determining the luminescence efficiency, energy transfer mechanisms, and overall performance of phosphor materials. In this regard, niobate-based compounds have gained attention due to their wide band gap, excellent chemical stability, and favorable optical properties [4]. $BaNb_2O_6$, in particular, is a promising host material due to its robust orthorhombic structure and the presence of NbO_6 octahedral units, which provide a stable environment for rare - earth ion incorporation. The strong Nb - O bonding network enhances structural rigidity and minimizes non-radiative losses, making it suitable for luminescent applications [5].

Despite these advantages, limited studies have been reported on Dy^{3+} - activated $BaNb_2O_6$ phosphors, especially concerning their photometric properties and decay behavior. Understanding concentration quenching mechanisms, lifetime characteristics, and chromaticity properties is essential for optimizing these materials for practical applications. Therefore, the present work focuses on the synthesis and comprehensive characterization of Dy^{3+} - doped $BaNb_2O_6$ phosphors, with emphasis on their structural, optical, luminescent, and photometric properties.

2. Experimental methodology

Dy^{3+} - doped $BaNb_2O_6$ phosphors were synthesized using a conventional solid-state reaction technique due to its simplicity and ability to produce highly crystalline materials. High-purity precursor materials, including barium carbonate

($BaCO_3$), niobium pentoxide (Nb_2O_5), and dysprosium oxide (Dy_2O_3), were used as starting materials. Stoichiometric amounts of these precursors were accurately weighed and thoroughly mixed using an agate mortar and pestle to achieve homogeneous blending. The mixture was then subjected to high-temperature calcination in a muffle furnace to facilitate solid-state diffusion and phase formation.

The structural properties of the synthesized phosphors were analyzed using X-ray diffraction (XRD), which provides information about crystal structure and phase purity (Rigaku). Fourier transform infrared (FTIR) spectroscopy was employed to identify functional groups and confirm the formation of NbO_6 units (Bruker Optik GmbH). Optical absorption properties were studied using UV - Vis diffuse reflectance spectroscopy (DRS), and the optical band gap was estimated using the Kubelka - Munk function (Agilent Cary Model 5000). Photoluminescence emission spectra were recorded under laser excitation to evaluate luminescent behavior, while decay kinetics were measured to determine lifetime characteristics (Agilent Cary Eclipse). Chromaticity coordinates, color purity and correlated color temperature (CCT) values were calculated using CIE analysis to assess photometric performance (ColorCalculator and GoCIE).

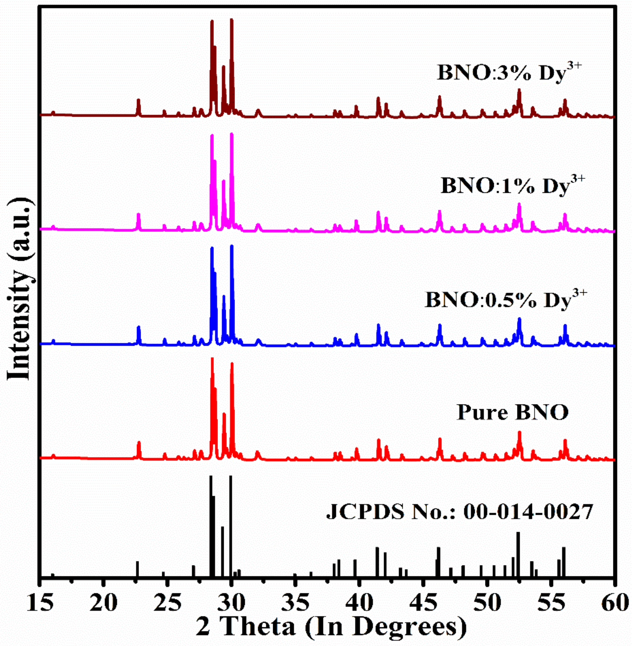

Figure 1: XRD patterns of $BaNb_2O_6$: xDy^{3+} (x = 0, 0.005, 0.01 and 0.03) Samples.

3. Results and Discussion

3.1 X-ray Diffraction

The XRD patterns of Dy^{3+} - activated $BaNb_2O_6$ phosphors confirm the formation of a well-crystallized orthorhombic phase consistent with standard $BaNb_2O_6$ diffraction data (JCPDS:14-0027) [6]. All observed diffraction peaks can be indexed to the host lattice without the appearance of any impurity peaks, indicating high phase purity. The absence of secondary phases confirms that Dy^{3+} ions are successfully incorporated into the $BaNb_2O_6$ lattice.

A careful examination of peak positions reveals no significant shift with increasing Dy^{3+} concentration, suggesting that the substitution of Dy^{3+} ions does not cause major lattice distortion. This behavior indicates that the host lattice has sufficient tolerance to accommodate Dy^{3+} ions. However, slight variations in peak intensity and broadening may be attributed to changes in crystallite size and local structural strain induced by dopant incorporation. The crystallite size, calculated using the Scherrer equation, falls within the nanometer range, which is beneficial for luminescence due to increased surface area and reduced scattering losses [6]. Further we have used Debye-Scherrer equation to calculate the crystallite size and is presented in Table no. 1.

Table 1: Crystallite size, lattice constants and cell volume of $BaNb_2O_6$: xDy^{3+} (x = 0, 0.01, 0.04, and 0.07) Samples.

Dy^{3+} Concentration (mol %)	**Average Crystallite Size (nm)**	**Lattice constants (Å)**			**Cell Volume (Å^3)**
		a	***b***	***c***	
0.5	68	12.092	10.199	7.909	977.559
1	67	12.119	10.300	7.900	978.098
2	63	12.200	10.256	7.899	976.978
3	69	12.129	10.255	7.852	978.009

Table 2: Chromaticity coordinates (x, y), CCT and Color Purity (CP) of BNO: Dy^{3+} phosphors.

Dy^{3+} concentrations (mol%)	**Chromaticity Coordinates**		**CCT(K)**	**Color Purity (%)**
	x	***y***		
0.5	0.3114	0.3172	6682	8.8
1	0.3161	0.3247	6351	6.5
2	0.3110	0.3162	6716	9.1
3	0.3097	0.3146	6813	9.6

3.2 FTIR Spectroscopy

The FTIR spectra provide important insights into the bonding environment of the synthesized phosphors. The presence of strong absorption bands below 1000 cm^{-1} confirms the formation of NbO_6 octahedral units, which are the fundamental structural units of $BaNb_2O_6$ [7]. The band observed around 833 cm^{-1} is attributed to Nb - O stretching vibrations, while bands near 595 cm^{-1} and 435 cm^{-1} correspond to Nb - O - Nb bending modes.

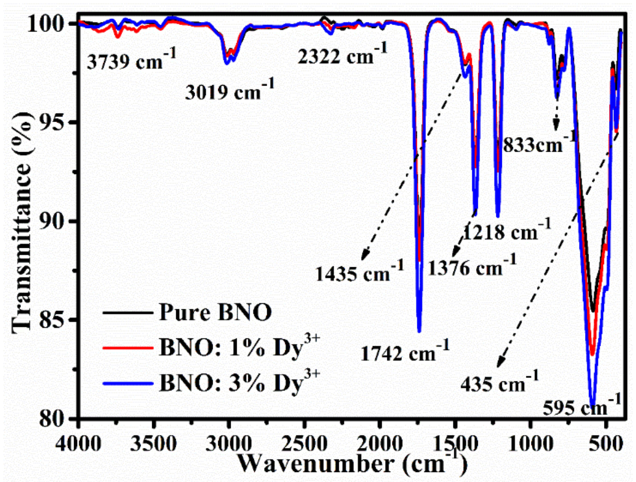

Figure 2: FTIR spectrum of pure BNO, BNO: 1% Dy3^+ and BNO: 3% Dy3^+ phosphors.

Weak absorption bands in the higher wavenumber region, particularly around 3739 cm^{-1}, are associated with O - H stretching vibrations due to adsorbed moisture. Additional minor bands may arise from residual carbonate groups. Importantly, no significant shift in peak positions is observed with increasing Dy^{3+} concentration, indicating that the incorporation of Dy^{3+} ions does not significantly alter the structural framework. This confirms the stability of the host lattice and supports the XRD findings [8].

3.3 UV-Vis Diffuse Reflectance Spectroscopy

The diffuse reflectance spectra of Dy^{3+} - doped $BaNb_2O_6$ phosphors exhibit strong absorption in the ultraviolet region, indicating efficient excitation under UV light. The reflectance decreases sharply in the UV region, which is characteristic of wide band gap materials [8].

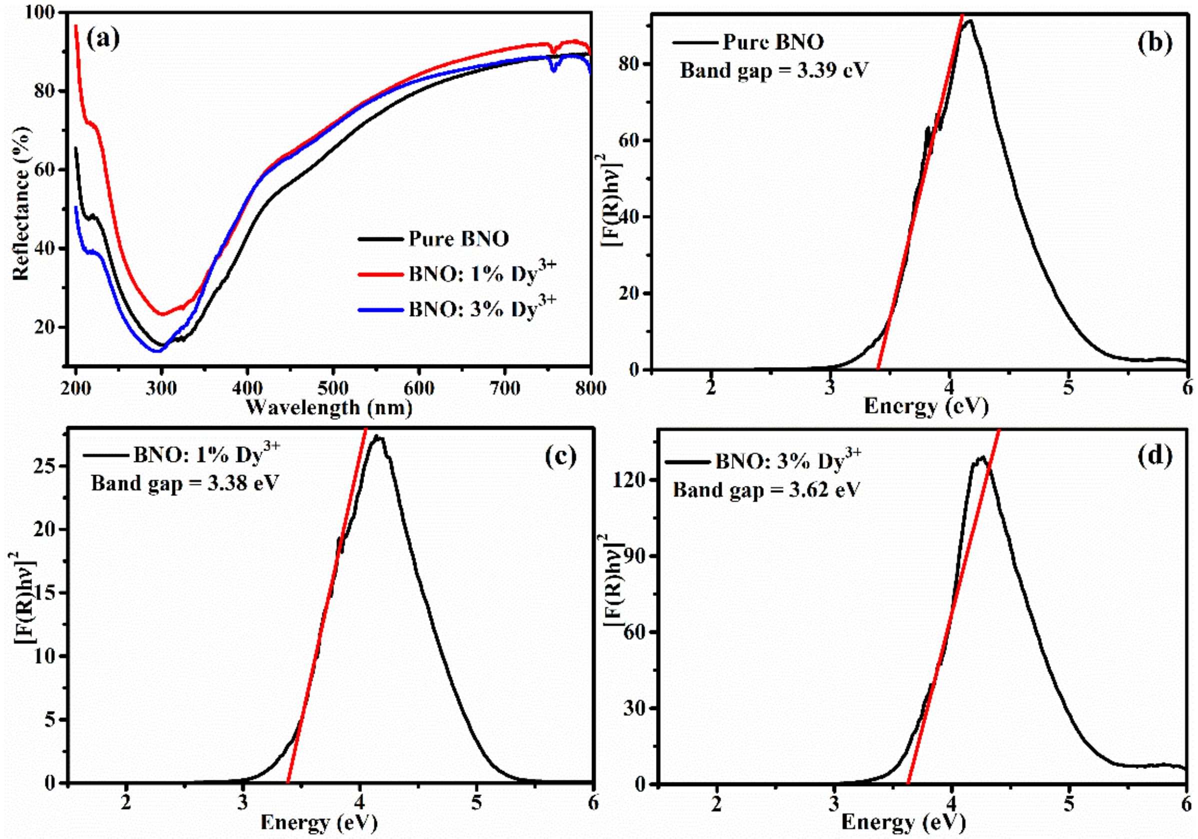

Figure 3: (a) Diffuse reflectance spectra and KM plots of (b) pure (c) 1 mol% (d) 3 mol%; Dy^{3+} doped SNO phosphor materials.

The optical band gap values were estimated using the Kubelka - Munk function and corresponding Tauc plots, which are widely used for band gap determination in powdered materials [7]. The band gap of the undoped sample is approximately 3.39 eV, which slightly decreases at lower Dy^{3+} concentrations and increases at higher concentrations, reaching around 3.62 eV. This variation can be attributed to the introduction of localized 4f energy levels and changes in the crystal field environment [9].

3.4 Photoluminescence Studies

The photoluminescence (PL) emission spectra of Dy^{3+} - activated $BaNb_2O_6$ phosphors under laser excitation exhibit well-defined characteristic transitions of Dy^{3+} ions, confirming the successful activation of luminescent centers within the host lattice. The emission spectrum is dominated by two main bands centered around ~ 480 nm and ~ 575 nm, which correspond to the $^4F_{9/2} \rightarrow {}^6H_{15/2}$ (blue) and $^4F_{9/2} \rightarrow {}^6H_{13/2}$ (yellow) transitions, respectively. Among these, the yellow emission is generally more intense due to its hypersensitive nature, which is strongly influenced by the local symmetry and crystal field environment around the Dy^{3+} ions [10].

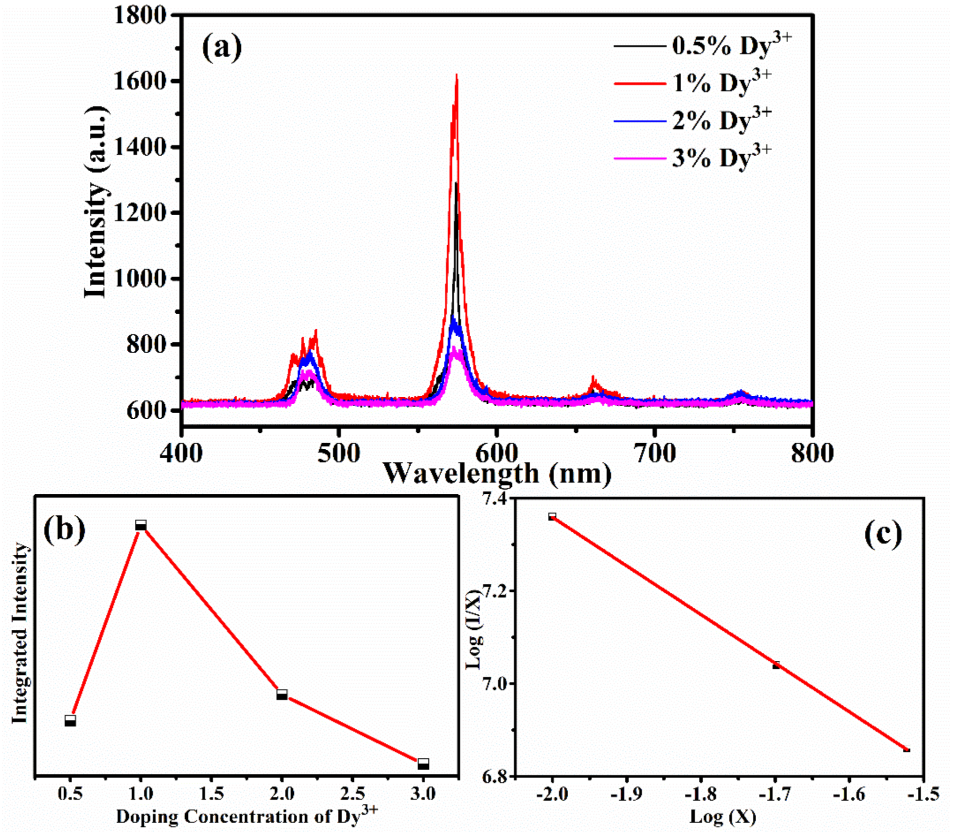

Figure 4: PL (a) Emission spectra; (b) Concentration quenching and (d) Plot of Log(X) vs. Log(I/X); of Dy^{3+} doped BNO phosphor materials.

The simultaneous presence of these two emission bands results in near - white light generation, which is highly desirable for single - phase white phosphor applications. The relative intensity ratio of blue to yellow emission plays a crucial role in determining the final emission color. In the present system, this ratio indicates a balanced contribution from both transitions, leading to emission in the cool white region [11].

With increasing Dy^{3+} concentration, the emission intensity initially increases, reaching a maximum at 1 mol% doping. This behavior is attributed to the increase in the number of luminescent centers, which enhances radiative recombination probability. However, beyond this optimal concentration, a gradual decrease in emission intensity is observed, indicating the onset of concentration quenching. This quenching effect arises due to the reduction in the average distance between Dy^{3+} ions, which facilitates non-radiative energy transfer processes.

The dominant quenching mechanism in such systems is typically governed by multipolar interactions, particularly dipole - dipole coupling, as described by Dexter's theory. At higher concentrations, excitation energy migrates between neighboring Dy^{3+} ions and is eventually dissipated through non-radiative pathways, leading to a reduction in emission efficiency [12]. Therefore, 1 mol% Dy^{3+} is identified as the optimal doping concentration for achieving maximum luminescence intensity in $BaNb_2O_6$ phosphors.

3.5 Decay Kinetics

The luminescence decay behavior of Dy^{3+} - doped $BaNb_2O_6$ phosphors provides important insights into the recombination dynamics of excited states and the efficiency of radiative processes. The decay curves recorded for the characteristic Dy^{3+} emissions were found to fit well with a single exponential function, indicating that the luminescence originates from a single type of emissive center within the host lattice. This suggests that Dy^{3+} ions occupy equivalent crystallographic sites and experience a relatively uniform local environment.

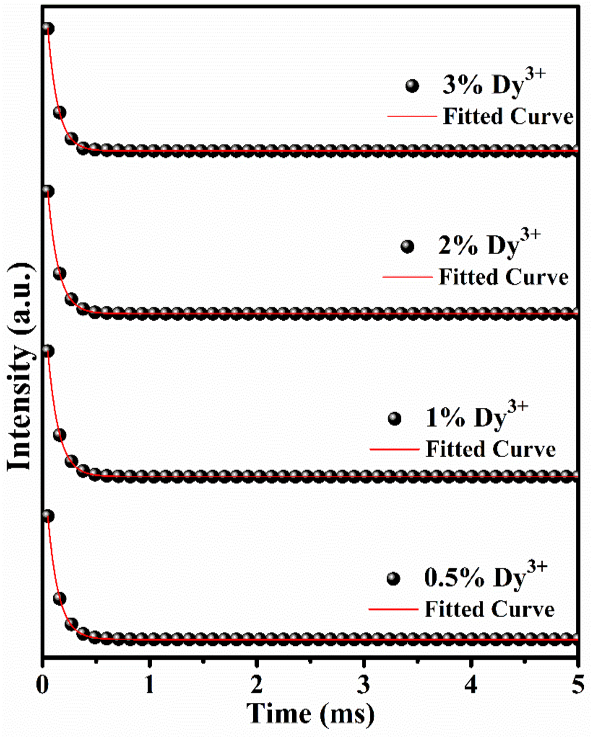

Figure 5: Decay curves for BNO: Dy^{3+} Phosphors.

The decay behavior can be described using relation [13]:

$$I = I_o e^{-\frac{t}{\tau}},$$

where $I(t)$ is the emission intensity at time t, I_o is the initial intensity, and τ is the decay lifetime.

The calculated lifetimes for the synthesized phosphors lie in the range of 0.09 - 0.1 ms, which is consistent with typical values reported for Dy^{3+} - activated oxide phosphors. A slight decrease in lifetime is observed with increasing Dy^{3+} concentration. This trend can be attributed to enhanced non-radiative energy transfer processes between closely spaced Dy^{3+} ions, which reduce the probability of radiative recombination.

The single exponential nature of the decay curves confirms that there is minimal contribution from defect-related or trap-assisted recombination processes, indicating good crystallinity and low defect density in the synthesized phosphors. Furthermore, the relatively short decay time is advantageous for practical applications, as it allows for faster response times and reduces afterglow effects in lighting devices [14]. The observed correlation between decreasing lifetime and concentration quenching behavior further supports the presence of energy transfer mechanisms such as dipole - dipole interactions, which become more significant at higher dopant concentrations.

3.6 Photometric properties

The photometric performance of Dy^{3+} - doped $BaNb_2O_6$ phosphors was evaluated using the Commission Internationale de l'Éclairage (CIE) 1931 chromaticity diagram, which provides a quantitative representation of the emitted color. The calculated chromaticity coordinates for all compositions are located in the cool white region of the CIE diagram, confirming the effective combination of blue and yellow emissions from Dy^{3+} ions.

One of the key observations is the minimal shift in chromaticity coordinates with increasing Dy^{3+} concentration, which indicates excellent color stability. This is an important requirement for practical lighting applications, where consistent color output is essential. The stable emission behavior suggests that the relative intensity ratio of blue and yellow transitions remains nearly constant across different doping levels.

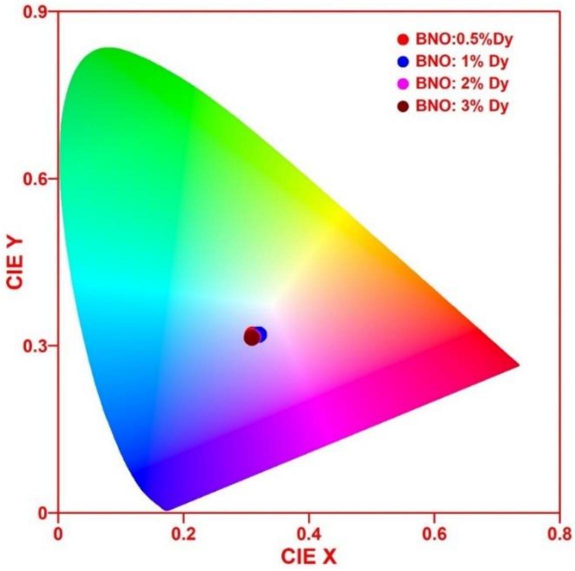

Figure 6: CIE diagrams for $BaNb_2O_6$: xDy^{3+} (x = 0.005, 0.01, 0.02 and 0.03) phosphors.

The color purity of the phosphors is found to be approximately 10%, which indicates a relatively broad emission spectrum. Although low color purity may seem disadvantageous for monochromatic applications, it is highly beneficial for white light generation, as it ensures better color mixing and improved visual comfort [15].

The temperature of an ideal blackbody radiator that emits light with a colour identical to the phosphor is represented by the correlated colour temperature (CCT) of a phosphor. The McCamy relation was used in this work to compute the CCT values. The correlated color temperature (CCT), calculated using standard empirical relations, is found to be greater than 5000 K for all compositions. This corresponds to cool white light, which is widely used in commercial lighting, office environments, and display backlighting. High CCT values indicate a higher contribution of blue emission, which enhances brightness and visual clarity [15].

The combination of suitable chromaticity coordinates, low color purity, and high CCT values demonstrates that Dy^{3+} - activated $BaNb_2O_6$ phosphors are capable of producing stable and efficient white light. These photometric characteristics, along with good structural and luminescent properties, make them strong candidates for application in phosphor-converted WLEDs.

4. Conclusions

Dy^{3+} - activated $BaNb_2O_6$ phosphors were successfully synthesized via a conventional solid-state reaction method and systematically investigated for their structural, optical, and luminescent properties. XRD analysis confirmed the formation of a single-phase orthorhombic structure with high crystallinity, while FTIR results verified the presence of NbO_6 octahedral units, indicating structural stability upon Dy^{3+} incorporation.

UV - Vis diffuse reflectance studies revealed strong absorption in the ultraviolet region with band gap values ranging from 3.38 to 3.62 eV, making the phosphors suitable for UV - excited applications. Photoluminescence analysis exhibited characteristic blue (~480 nm) and yellow (~ 575 nm) emissions of Dy^{3+} ions, resulting in near-white light emission. The emission intensity reached a maximum at 1 mol% Dy^{3+} concentration and decreased thereafter due to concentration quenching governed by non-radiative energy transfer through dipole - dipole interactions.

The decay curves followed a single exponential behavior with lifetimes in the range of 0.09 - 0.1 ms, indicating a uniform luminescent environment. Photometric analysis confirmed emission in the cool white region with a color purity of ~10% and correlated color temperature (CCT) values above 5000 K, along with good color stability.

Overall, the results demonstrate that Dy^{3+} - doped $BaNb_2O_6$ phosphors exhibit favorable luminescent and photometric properties, making them promising candidates for solid-state lighting and white LED applications.

Acknowledgements

The authors acknowledge the central research facility, IIT (ISM) Dhanbad.

Authors' contributions

Chandni Kumari – Study conception and design, data analysis and manuscript writing.

Praveen Kumar Vishwakarma– Sample preparation, data collection and analysis.

The authors read and approved the final manuscript.

Conflicts of interest

The authors do not have any financial interest or personal relationship that can influence this work.

Funding

This research received no external funding.

Data availability

The data are presented in the manuscript.

References

[1] G. Blasse, B.C. Grabmaier, Luminescent Materials, Springer, Berlin, Heidelberg (1994).
[2] W.M. Yen, S. Shionoya, H. Yamamoto (Eds.), Phosphor Handbook, CRC Press/Taylor & Francis, Boca Raton (2007).
[3] R. Tang, Y. Liu, C. Zhu, J. Zhu, G. Yu, Crystal structure and luminescence properties of rare-earth-doped intermetallic compounds, *Intermetallics* **14** (2006) 361–366.
[4] P. Dorenbos, Energy of the first 4f7→4f65d transition of Eu^{2+} in inorganic compounds, *J. Lumin.* **104** (2003) 239–260.
[5] A.K. Vishwakarma, K. Jha, M. Jayasimhadri, A.S. Rao, K. Jang, B. Sivaiah, D. Haranath, Structural and luminescence properties of rare-earth activated phosphors, *J. Alloys Compd.* **622** (2015) 97–103.
[6] B.D. Cullity, Elements of X-Ray Diffraction, Addison-Wesley Publishing Company, Inc., Reading, MA (1978).
[7] K. Nakamoto, Infrared and Raman Spectra of Inorganic and Coordination Compounds, Wiley, Hoboken, NJ (2008).
[8] A.K. Vishwakarma, M. Jayasimhadri, Luminescence characteristics of rare-earth doped phosphors, *J. Lumin.* **176** (2016) 112–118.
[9] S. Jana, A. Mondal, J. Manam, S. Das, Structural and optical investigations of phosphor materials, *J. Alloys Compd*. **821** (2020) 153227.
[10] C. Kumari, J. Manam, S.K. Sharma, Optical and luminescence properties of rare-earth activated phosphors, *J. Mater. Sci.* **60** (2025) 11311–11325.
[11] A. Kumar, J. Manam, Photoluminescence and structural studies of phosphor materials, *Opt. Mater*. **96** (2019) 109327.
[12] S. Yadav, D. Kumar, R.S. Yadav, S.B. Rai, A.K. Singh, Luminescence investigations of rare-earth doped ceramic phosphors, *Ceram. Int*. **48** (2022) 30754–30763.
[13] C. Kumari, J. Manam, S.K. Sharma, Structural, thermal and optical properties of phosphor materials, *Mater. Sci. Semicond. Process*. **158** (2023) 107363.
[14] C. Kumari, R. Gopal, H. Yadav, J. Manam, Optical behaviour of rare-earth doped phosphor materials, *J. Mater. Sci.: Mater. Electron.* **35** (2024) 1045.
[15] R. Gopal, A. Kumar, J. Manam, Luminescence and structural investigations of inorganic phosphors, *Mater. Chem. Phys*. **272** (2021) 124969.